Theoretical study of aluminum arsenide clusters: Equilibrium geometries and electronic structures of Al_nAs_n ($n = 1$–4)

Yuhui Qu [a,*], Wanyong Ma [a], Xiufang Bian [b],
Hongwei Tang [b], Weixing Tian [b]

[a] Department of Chemistry, Shandong Institute of Light Industry, Shandong, Jinan 250100, PR China
[b] Key Laboratory of Liquid Structure and Heredity of Materials, Ministry of Education, Shandong University, Shandong, Jinan 250061, PR China

Abstract

The geometry, electronic configurations, harmonic vibrational frequencies and stability of the structural isomers of Al_nAs_n clusters ($n = 1$–4) have been investigated using density functional theory. For dimers and trimers, the lowest energy structures are planar cumulenic rings (IIs, VIs) with D_{nh} symmetry. The caged structure with T_d symmetry (IXs) lie lowest in energy among the tetramers. The Al–As bond dominates the structures for many isomers so that one preferred dissociation channel is loss of the AlAs monomer. The atomic charges, hybridization and chemical bonding in the different structures are also discussed. Comparisons with valence-isoelectronic Si_{2n}, Al_nP_n and Ga_nAs_n clusters of same size, the properties of the aluminum arsenide clusters are analogous to those of their corresponding Al_nP_n, Si_{2n} counterparts. The results can explain the modification and refinement of Si phase in Al–Si alloy in the molecular level.

1. Introduction

In recent years, a number of theoretical and experimental studies of the structures and properties of mixed clusters has become a subject of academic, scientific and technological interest. Among them, the spectroscopy and electronic structure of semiconductor clusters, especially the group IV semicon- ductor clusters, and the group III–V clusters are becoming increasingly technologically important [1–31] as the group III–V semicon- ductors are used in the fabrication of fast micro-electronic devices. The knowledge of the physical and chemical properties of these materials at the molecular level can be vital in improving the device preparation processes, such as the sputtering process by which the surface layers of the electronic devices are generally constructed [32–34]. Among the group III–V clusters, gallium arsenide has received a significant amount of interest from both theoretical and experimental scientists [5–19]. The aluminum arsenide clusters have been the focus of a few experimental and theoretical studies, but in a limited way [13,19]. No theoretical

study has been devoted to Al_nAs_n ($n = 1$–4) clusters, to the best of our knowledge. In addition, the similarities and differences between mixed group III–V clusters and those of carbon or silicon clusters are also important aspects which need to be investigated. My motivations for the study of Al_nAs_n clusters is as a comparison with the recently results from a number of group III–V clusters, such as Al_nP_n and Ga_nAs_n clusters [5–20]. Aluminum and arsenic are also a group III–V atoms. Consideration of electronic structure, independent of atomic size, would lead to the conclusion that the Al_nAs_n clusters might be analoge to Al_nP_n and Ga_nAs_n clusters of same size. Computational studies are a means to explore this possibility. Finally, the study of clusters provides a means to develop an understanding of the nucleation transition of gas-phase species into the condensed phase.

Our research group has initiated a theoretical study on the structures and energies of AlAs mixed clusters in the frame-work of density functional theory. In particular, we have studied the monomer, dimers, trimers and tetramers of AlAs. This paper is organized as follows. In Section 2, details of the comp- utational techniques employed in this study are given. Results are presented and discussed in Section 3, where we discuss the geometric structures, electronic configurations, harmonic

vibrational frequencies, and cluster stabilities. Chemical bonding of the lowest energy Al_nAs_n clusters are also discussed in this section. We give a summary and conclusions of the present study in Section 4.

2. Computational methods

The geometrical parameters for several different starting structural and electronic (singlet, triplet) arrangements were optimized completely using the density functional theory (DFT) selecting the Becke's non-local three-parameter hybrid func-

tional combined with the Lee–Yang–Parr correlation functional (B3LYP) method [35–38] by means of efficient gradient techniques with the 6-31G(d) basis set. The geometries were then refined with the 6-311++G(2d,2p) basis set. The configuration was regarded as optimized when the maximum force, the root mean square (rms) force, the maximum displacement of atoms, and the rms displacement of atoms have magnitudes less than 0.00045 a.u., 0.0003 a.u., 0.0018 a.u. and 0.0012 a.u., respectively. In addition, the nature of the stationary points were determined in all cases by the analytical evaluation of the complete matrix of force constants and the associated harmonic vibrational frequencies at its corresponding level of theory. This enables us to verify that they correspond to true minima on the potential surface, and also to estimate the zero-point vibrational energy (ZPVE) correction. In order to compute accurate relative energies, additional single point energy calculations were carried out for all the low-energy isomers by means of complete fourth-order Moller–Plesset perturbation theory using the 6-311++G(2d,2p) basis set (MP4(SDTQ)/6-311++G(2d,2p)// B3LYP/6-311++G(2d,2p)) [39], which has contributions from single, double, triple and quadruple excitations from the starting HF wave function [40]. The atomic charges, valence orbital hybridizations and chemical bonding for the lowest energy clusters have been calculated using natural bond orbital analysis (NBO, Version 3) [41–48]. This method using natural population analysis [49–51], unlike Mulliken population analysis which
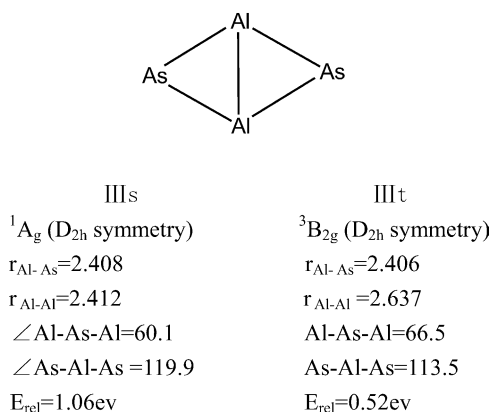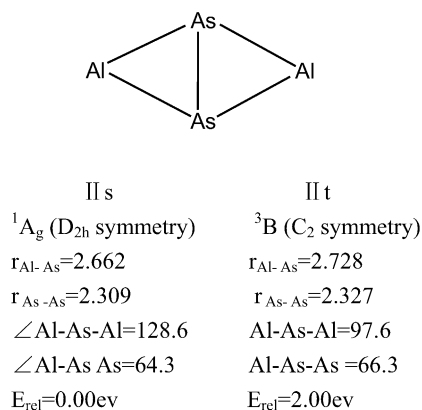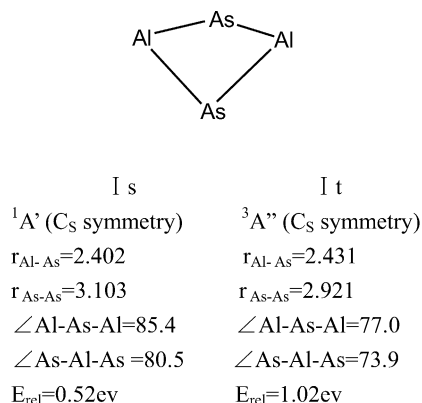

I s	I t
$^1A'$ (C_S symmetry)	$^3A''$ (C_S symmetry)
$r_{Al\text{-}As}$=2.402	$r_{Al\text{-}As}$=2.431
$r_{As\text{-}As}$=3.103	$r_{As\text{-}As}$=2.921
$\angle$Al-As-Al=85.4	$\angle$Al-As-Al=77.0
$\angle$As-Al-As=80.5	$\angle$As-Al-As=73.9
E_{rel}=0.52ev	E_{rel}=1.02ev

II s	II t
^1A_g (D_{2h} symmetry)	^3B (C_2 symmetry)
$r_{Al\text{-}As}$=2.662	$r_{Al\text{-}As}$=2.728
$r_{As\text{-}As}$=2.309	$r_{As\text{-}As}$=2.327
$\angle$Al-As-Al=128.6	Al-As-Al=97.6
$\angle$Al-As As=64.3	Al-As-As =66.3
E_{rel}=0.00ev	E_{rel}=2.00ev

As———Al———Al———As	

IVs	IVt
$^1\Sigma g$ ($D_{\infty h}$ symmetry)	$^3\Sigma g$ ($D_{\infty h}$ symmetry)
$r_{Al\text{-}As}$=2.262	$r_{Al\text{-}As}$=2.284
$r_{Al\text{-}Al}$=2.511	$r_{Al\text{-}Al}$=2.468
$\angle$As-Al-Al=180.0	As-Al-Al=180.0
E_{rel}=3.24ev	E_{rel}=3.34ev

IIIs	IIIt
^1A_g (D_{2h} symmetry)	$^3B_{2g}$ (D_{2h} symmetry)
$r_{Al\text{-}As}$=2.408	$r_{Al\text{-}As}$=2.406
$r_{Al\text{-}Al}$=2.412	$r_{Al\text{-}Al}$=2.637
$\angle$Al-As-Al=60.1	Al-As-Al=66.5
$\angle$As-Al-As =119.9	As-Al-As=113.5
E_{rel}=1.06ev	E_{rel}=0.52ev

V t
$^3A''$ (C_S symmetry)
$r_{Al\text{-}As}$=2.457
$r_{Al\text{-}Al}$=3.482
$\angle$As-Al-As=95.3
$\angle$Al-As-Al=177.0
E_{rel}=1.47ev

Fig. 1. Isomeric structures for rhombic Al_2As_2. Geometric parameters are summarized and the energy, relative to the minimum energy structure is presented. Detailed geometries will be provided upon request.
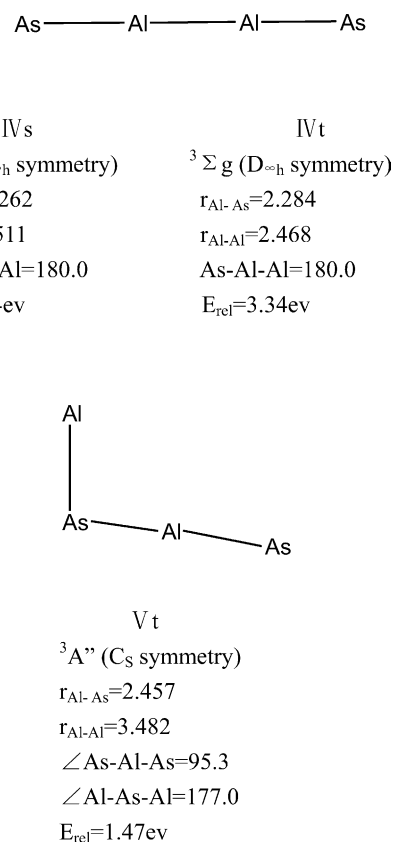
Fig. 2. Isomeric structures for linear and bent Al_2As_2. Geometric parameters are summarized and the energy, relative to the minimum energy structure is presented. Detailed geometries will be provided upon request.

substantially underestimates the ionicity of molecules involving large electronegativity differences, gives a reasonable physical picture of the charge contribution while being relatively insensitive to the basis set size. All calculations reported in this work were carried out with the Gaussian-03 program package [52].

3. Results and discussion

3.1. Geometry optimization

We have searched for different isomers on both the singlet and triplet Al_nAs_n potential surfaces, but only true minima with all their vibrational frequencies real will be shown. The optimized geometrical data at the B3LYP/6-311++G(2d,2p) levels and pictorial representations for all isomers and spin states examined are shown in Figs. 1–4. Table 1 lists the bonding energies with respect to reference fragments, which in our case are the atoms. The vibrational frequencies are given in Table 2.

3.1.1. AlAs

We have included electronic structure calculations on the monomer for comparison. The results indicate that the lowest

energy structure corresponds to a molecule in a $^3\Sigma$ state with a bond length of 2.327 Å. The lowest singlet state, $^1\Sigma$, lies 0.53 eV above the triplet ground state and has a compressed bond length, relative to the triplet state, of 2.180 Å. The calculated harmonic frequency are 442 cm^{-1} and 362 cm^{-1}, respectively.

Natural population analysis yields atomic charges of +0.55e on Al and −0.55e on As, consistent with the electronegativity difference between the elements. Since both Al and As are trivalent elements, the atomic charges of only 0.55e indicate significant covalent contribution to the bonding. Examination of the MO composition of the molecule can also provides some indication. If the molecule is in the z-axis, the valence electron
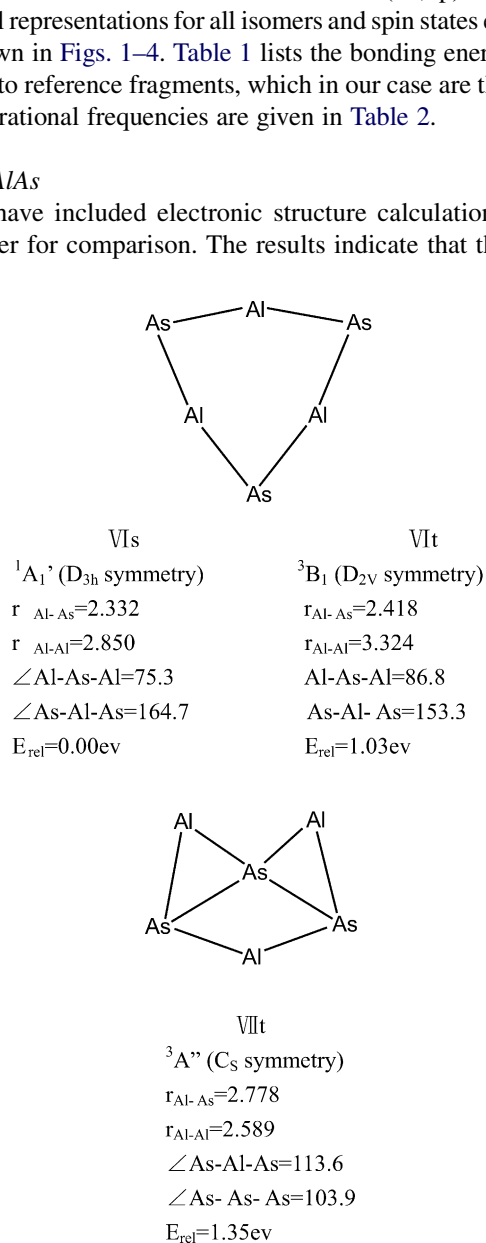

VIs
$^1A_1'$ (D$_{3h}$ symmetry)
r $_{Al-As}$=2.332
r $_{Al-Al}$=2.850
∠Al-As-Al=75.3
∠As-Al-As=164.7
E$_{rel}$=0.00ev

VIt
$^3B_1$ (D$_{2V}$ symmetry)
r$_{Al-As}$=2.418
r$_{Al-Al}$=3.324
Al-As-Al=86.8
As-Al-As=153.3
E$_{rel}$=1.03ev

VIIt
$^3A''$ (C$_S$ symmetry)
r$_{Al-As}$=2.778
r$_{Al-Al}$=2.589
∠As-Al-As=113.6
∠As-As-As=103.9
E$_{rel}$=1.35ev

Fig. 3. Isomeric structures for Al$_3$As$_3$. Geometric parameters are summarized and the energy, relative to the minimum energy structure is presented. Detailed geometries will be provided upon request.
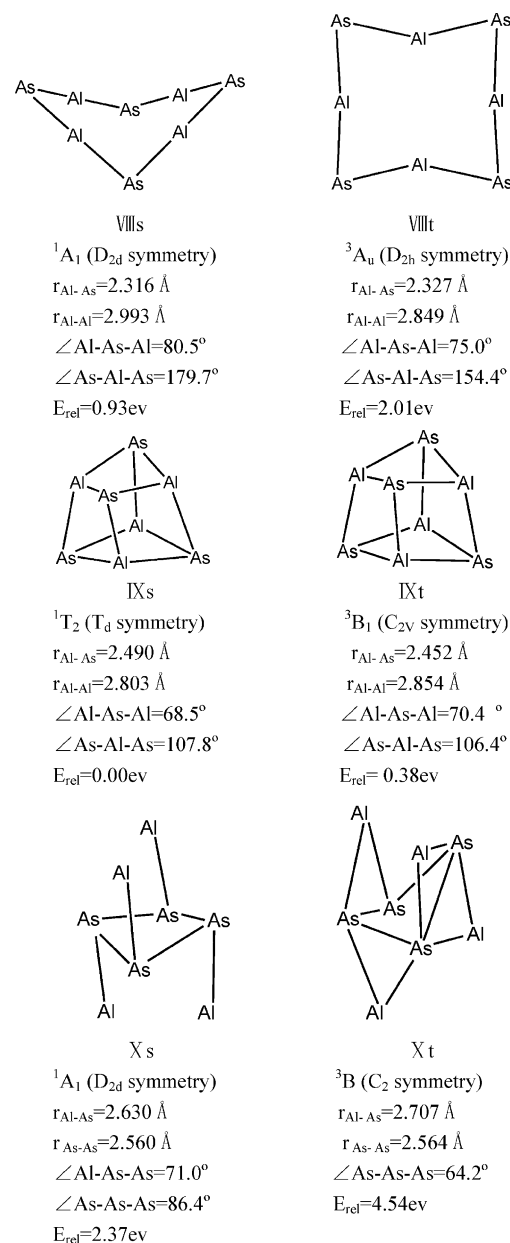
VIIIs
$^1A_1$ (D$_{2d}$ symmetry)
r$_{Al-As}$=2.316 Å
r$_{Al-Al}$=2.993 Å
∠Al-As-Al=80.5°
∠As-Al-As=179.7°
E$_{rel}$=0.93ev

VIIIt
^3A_u (D$_{2h}$ symmetry)
r$_{Al-As}$=2.327 Å
r$_{Al-Al}$=2.849 Å
∠Al-As-Al=75.0°
∠As-Al-As=154.4°
E$_{rel}$=2.01ev

IXs
$^1T_2$ (T$_d$ symmetry)
r$_{Al-As}$=2.490 Å
r$_{Al-Al}$=2.803 Å
∠Al-As-Al=68.5°
∠As-Al-As=107.8°
E$_{rel}$=0.00ev

IXt
$^3B_1$ (C$_{2V}$ symmetry)
r$_{Al-As}$=2.452 Å
r$_{Al-Al}$=2.854 Å
∠Al-As-Al=70.4 °
∠As-Al-As=106.4°
E$_{rel}$= 0.38ev

X s
$^1A_1$ (D$_{2d}$ symmetry)
r$_{Al-As}$=2.630 Å
r$_{As-As}$=2.560 Å
∠Al-As-As=71.0°
∠As-As-As=86.4°
E$_{rel}$=2.37ev

X t
^3B (C$_2$ symmetry)
r$_{Al-As}$=2.707 Å
r$_{As-As}$=2.564 Å
∠As-As-As=64.2°
E$_{rel}$=4.54ev

Fig. 4. Isomeric structures for Al$_4$As$_4$. Geometric parameters are summarized and the energy, relative to the minimum energy structure is presented. Detailed geometries will be provided upon request.

Table 1
Bonding energies (eV) for aluminum arsenide clusters

Cluster	Structure	Point group	Spin	B3LYP/6-311++G(2d,2p)	MP4(SDTQ)/6-311++G(d,p)//B3LYP/6-311++G(2d,2p)	ZPVE (eV)
Al_2As_2	Is	C_S	0	10.49	10.94	0.091
	It	C_S	1	10.35	10.44	0.095
	IIs	D_{2h}	0	11.24	11.46	0.076
	IIt	C_2	1	10.33	9.46	0.058
	IIIs	D_{2h}	0	10.29	10.40	0.10
	IIIt	D_{2h}	1	10.93	10.94	0.094
	IVs	$D_{\infty h}$	0	8.05	8.22	0.085
	IVt	$D_{\infty h}$	1	8.79	8.12	0.080
	Vt	C_S	1	10.10	9.99	0.075
Al_3As_3	VIs	D_{3h}	0	18.50	18.87	0.18
	VIt	C_{2V}	1	17.72	17.84	0.15
	VIIt	C_S	1	17.41	17.52	0.15
Al_4As_4	VIIIs	D_{2d}	0	25.66	26.20	0.25
	VIIIt	D_{2h}	1	24.90	25.12	0.23
	IXs	T_d	0	26.14	27.13	0.28
	IXt	C_{2V}	1	25.76	26.75	0.26
	Xs	D_{2d}	0	23.72	24.76	0.18
	Xt	C_{2h}	1	24.14	22.59	0.20

configuration is $10(\sigma)^2$, $11(\sigma)^2$, $9(\pi)^2$, $10(\pi)^2$. Here, 9π and HOMO are bonding π orbital, consisting of p-orbitals in the x-axis and y-axis, respectively, involving arsenic orbitals and contribution from the alluminum atom. Therefore, the molecule can be considered as triple bond.

3.1.2. Al_2As_2 isomers

We have examined possible structural isomers for the dimer: rhombic forms of As–Al–As–Al (I, II and III), linear As–Al–Al–As (IV) and bent As–Al–As–Al (V). The lowest energy structure (IIs) corresponds to a totally symmetric singlet state with a rhombus geometry in which the arsenic atoms lie along the short diagonal. This D_{2h} structure is labeled IIs and has a ^1A_g electronic state. In this configuration, the As–As and Al–As distances are 2.309 Å and 2.662 Å, respectively. The Al–As–Al angle is 128.6° and the Al–As–As angle is 64.3°. In this configuration, the Al–As bond length in IIs is significantly elongated in comparison with the monomer. The overall structure is best classified as alluminum end-capped As_2. If the molecule is in the yz plane with the y-axis along the short diagonal, the valence electron configuration is {core} $(a_g)^2$ $(b_{2u})^2$ $(b_{1u})^2$ $(a_g)^2$ $(a_g)^2$ $(b_{3u})^2$ $(b_{3g})^2$ $(b_{1u})^2$. Here, b_{3u} is a bonding π orbital, consisting of out-of-plane p_x-orbitals, involving principally two arsenic atoms. Thus, the As–As bond can be considered as double bond. Both the rhombus geometry and the orbital configuration are exactly analogous to those of the valence-isoelectronic Si_4 [1], Al_2P_2 [16,20] and Ga_2As_2 [7] molecules. However, the strong As–As bonding existed both in Al_2P_2 and in Ga_2As_2 differs from the rather weak Si–Si bonding across the short diagonal in Si_4. Natural population analysis yields atomic charges of ±0.50e, showing slightly smaller charge separation than in diatomic AlAs. The importance of As–As bonding is evident when the As–As distance is systematically increased while the Al–Al bond length is decreased. Optimization of the structure which involves an Al–Al bond along the short axis (IIIs) results in a molecule of significantly 1.06 eV higher in energy than IIs. This configuration also has D_{2h} symmetry and a ^1A_g electronic state. However, the valence electron orbital configuration is different {core} $(a_g)^2$ $(b_{1u})^2$ $(a_g)^2$ $(b_{2u})^2$ $(b_{3g})^2$ $(b_{3u})^2$ $(b_{1u})^2$ $(b_{2g})^2$. The lowest-lying triplet state is obtained upon $2b_{2g} \rightarrow 9a_g$ excitation with Al–As bond length (2.406 Å) somewhat longer than that in the monomer and an Al–Al distance (2.637 Å). Finally, a starting geometry intermediate between these two extremes results in an optimized structure (Is) with Al–As bond length (2.402 Å) slightly longer than that in the monomer and an As–As distance (3.103 Å). For linear configuration, the structure with alternating bent structure was energetically preferred to the structure with Al–Al bond. This is attributed to the strength of the Al–As bond relative to that of Al–Al. These triplet states are 0.50 eV (It), 2.00 eV (IIt) and 0.10 eV (IVt), respectively, lower in energy than the corresponding singlet states. These isomers are found to be minima, as seen from the vibrational frequencies listed in Table 2.

3.1.3. Al_3As_3 isomers

The hexagonal structure (VIs) has D_{3h} symmetry. In this structure, the three arsenic atoms are edge capping the triangle formed from the three alluminum atoms. The optimized Al–Al and Al–As internuclear distances are 2.850 Å and 2.332 Å, respectively. The Al–As bond length is longer than that observed in the monomer (2.327 Å). An alternative interpretation of this structure is as a pair of concentric Al_3 and As_3 triangles. The lowest-lying singlet state electronic configuration is {core} $(a_1')^2$ $(e')^4$ $(a_1')^2$ $(e')^4$ $(a_2')^2$ $(a_2'')^2$ $(e')^4$ $(e'')^4$. The lowest-lying triplet state is obtained upon $6e'' \rightarrow 9a_1'$ excitation. The singlet state lies approximately 1.03 eV below

Table 2
The harmonic vibrational frequencies calculated at the B3LYP/6-311++G(2d,2p) level

Cluster	Structure	Point group	Vibrational frequencies (cm^{-1})
Al$_2$As$_2$	Is	C$_S$	**111(a′)**, **143(a′)**, **239(a″)**, **292(a″)**, **323(a′)**, **363(a′)**
	It	C$_S$	**132(a′)**, **172(a′)**, **217(a″)**, **300(a′)**, **355(a″)**, **361(a′)**
	IIs	D$_{2h}$	**72(b$_{3u}$)**, **128(b$_{2u}$)**, 176(b$_{3g}$), 251(a$_g$), **265(b$_{1u}$)**, 333(a$_g$)
	IIt	C$_2$	**12(a)**, **63(b)**, **73(a)**, **228(a)**, **235(b)**, **319(a)**
	IIIs	D$_{2h}$	**127(b$_{3u}$)**, 225(a$_g$), 233(b$_{3g}$), **235(b$_{2u}$)**, **394(b$_{1u}$)**, 431(a$_g$)
	IIIt	D$_{2h}$	**91(b$_{3u}$)**, **177(b$_{2u}$)**, 210(a$_g$), 323(b$_{3g}$), **344(b$_{1u}$)**, 374(a$_g$)
	IVs	D$_{∞h}$	**28(π$_u$)**, **35(π$_g$)**, 85(π$_g$), 102(π$_g$), 148(σ$_g$), **413(σ$_u$)**, 554(σ$_g$)
	IVt	D$_{∞h}$	**33(π$_u$)**, **33(π$_u$)**, 84(π$_g$), 84(π$_g$), 152(σ$_g$), **378(σ$_u$)**, 522(σ$_g$)
	Vt	C$_S$	**47(a′)**, **87(a′)**, **116(a′)**, **202(a′)**, **273(a′)**, **479(a′)**
Al$_3$As$_3$	VIs	D$_{3h}$	62(e″), 62(e″), **117(a$_2''$)**, **157(e′)**, **157(e′)**, **209(e′)**, **209(e′)**, 227(a$_1$'), 292(a$_1'$), 419(a$_2'$), **502(e′)**, **502(e′)**
	VIt	C$_{2V}$	75(a$_2$), **85(b$_2$)**, **90(b$_1$)**, **99(a$_1$)**, **118(b$_1$)**, **150(b$_2$)**, **172(a$_1$)**, **205(a$_1$)**, **224(a$_1$)**, **390(b$_2$)**, **434(a$_1$)**, **436(b$_2$)**,
	VIIt	C$_S$	**34(a″)**, **88(a″)**, **98(a′)**, **145(a′)**, **161(a′)**, **179(a″)**, **186(a′)**, **258(a′)**, **287(a′)**, **287(a″)**, **345(a′)**, **347(a″)**
Al$_4$As$_4$	VIIIs	D$_{2d}$	34(a$_1$), **55(b$_2$)**, 86(b$_1$), **97(e)**, **97(e)**, 100(a$_2$), **147(b$_2$)**, **178(e)**, **178(e)**, 191(a$_1$), **194(b$_1$)**, **212(e)**, **212(e)**, 238(a$_1$), 465(a$_2$), **616(e)**, **616(e)**, **626(b$_2$)**
	VIIIt	D$_{2h}$	31(a$_g$), 32(a$_u$), **92(b$_{3u}$)**, **99(b$_{3u}$)**, 100(b$_{2g}$), 108(b$_{2g}$), 119(b$_{1g}$), **130(b$_{2u}$)**, **144(b$_{1u}$)**, 174(a$_g$), **194(b$_{1u}$)**, 194(a$_g$), **215(b$_{2u}$)**, 299(a$_g$), **410(b$_{1u}$)**, **440(b$_{2u}$)**, 442(b$_{3g}$), 495(b$_{3g}$)
	IXs	T$_d$	128(e), 128(e), **151(t$_2$)**, **151(t$_2$)**, **151(t$_2$)**, 217(a$_1$), 231(t$_1$), 231(t$_1$), 231(t$_1$), **258(t$_2$)**, **258(t$_2$)**, **258(t$_2$)**, 276(e), 276(e), 358(a$_1$), **389(t$_2$)**, **389(t$_2$)**, **389(t$_2$)**
	IXt	C$_{2V}$	**104(a$_1$)**, 117(a$_2$), **147(a$_1$)**, **148(b$_1$)**, 156(b$_2$), **172(a$_1$)**, **205(b$_1$)**, **218(a$_1$)**, 228(a$_2$), **230(b$_2$)**, **231(b$_1$)**, 276(a$_2$), **288(a$_1$)**, **298(b$_2$)**, **321(a$_1$)**, **334(b$_1$)**, **368(b$_2$)**, **383(a$_1$)**
	Xs	D$_{2d}$	**74(e)**, **74(e)**, 74(b$_1$), 86(a$_2$), **110(e)**, **110(e)**, 112(a$_1$), **121(b$_2$)**, 159(a$_1$), **179(e)**, **179(e)**, **181(b$_2$)**, 217(a$_1$), **224(e)**, **224(e)**, 230(b$_1$), **241(b$_2$)**, 265(a$_1$),
	Xt	C$_2$	**52(a)**, **59(b)**, **62(a)**, **114 (b)**, **133(a)**, **139(b)**, **144(a)**, **144(b)**, **167(a)**, **196(a)**, **197(b)**, **216(a)**, **238(a)**, **239(b)**, **247(b)**, **260(a)**, **290(a)**, **312(b)**

IR active modes are noted in bold.

the corresponding triplet state. Examination of the MO composition of the isomers provides some indication of the rationale leading to the calculated ground states. For *n* = 3, it is only for the cyclic structure and then only for the singlet electronic state, that a HOMO consisting of out-of-plane p-orbitals, involving mostly arsenic orbitals with a small contribution from the alluminum atom, is available. The ground state structure, therefore, exhibits what might be described as a pseudo-π orbital system which confers additional stability to the ring conformer. In VIs, the atomic charges of ±0.80e, indicating the ionic character of this two-dimensional structure. The geometry and orbital configuration of VIs are analogous to that in the system Al$_3$P$_3$ [16,20]. In order to assess the importance of aluminum–aluminum interaction, the Al–Al separation was increased while simultaneously decreasing the As–As distance. The energy increases as these distances are changed and a stationary point (VIIt) is located 0.32 eV above the isomer (VIt). The indication is that Al–Al interaction is significant and contributes to the stabilization of this geometry. A singlet for structure VIIs located with a imaginary frequency will not be discussed.

3.1.4. Al$_4$As$_4$ isomers

The optimized lowest energy structure of Al$_4$As$_4$ is a three-dimensional cubic form (T$_d$ symmetry) with two interpenetrating Al$_4$ and As$_4$ tetrahedrons in the singlet electronic state (IXs). The lowest-lying singlet state electronic configuration is {core} (a$_1$)^2 (t$_2$)^6 (a$_1$)^2 (t$_2$)^6 (e)^4 (t$_2$)^6 (t$_1$)^6. In this configuration, the Al–Al and Al–As distances are 2.803 Å and 2.490 Å, respectively. The Al–As–Al angle is 68.5° and the As–Al–As angle is 107.8°. Both the geometry and the orbital configuration are exactly analogous to those of the valence-isoelectronic Si$_8$ [1] and Al$_4$P$_4$ [16,20] molecules. The lowest-lying triplet state is obtained upon 7t$_1$ → 15a$_1$ excitation. This C$_{2V}$ structure is labeled as IXt and has a ^{3}B$_1$ electronic state. Natural population analysis indicated that the charges on the atoms are much larger (±0.71e). Thus, the electrostatic factors play a much larger factor. The hybridization on the Al atoms is 3s$^{1.00}$ 3p$^{1.23}$, as shown in Table 3. This can be considered as resulting from the interaction of promoted (s^{1}p^2) Al atoms with As atoms. The resulting stronger interaction partially offsets the promotion energy required. The charge flow from Al to As along the σ bond, thus, if we interact four Al atoms (s^{1}p^{1}p^1) with four As

Table 3
Valence natural orbital configurations[a] for the different atoms calculated at B3LYP/6-311++G(2d,2p) level

Cluster	Structure	Point group	Atom(s)	Hybridization	Natural charge
AlAs ($^3\Sigma$)		$C_{\infty v}$	Al	$s^{1.62} p^{0.81}$	0.55
			As	$s^{1.91} p^{3.60}$	−0.55
$Al_2As_2(^1A_g)$	IIs	D_{2h}	Al	$s^{1.89} p^{0.59}$	0.50
			As	$s^{1.83} p^{3.61}$	−0.50
$Al_3As_3(^1A_1')$	VIs	D_{3h}	Al	$s^{0.98} p^{1.17}$	0.80
			As	$s^{1.75} p^{3.98}$	−0.80
$Al_4As_4(^1T_2)$	IXs	T_d	Al	$s^{1.00} p^{1.23}$	0.71
			As	$s^{1.74} p^{3.88}$	−0.71

[a] Contributions from 4s, 3d and 4p are very small (<0.05) and will be ignored.

atoms ($s^2 p_x^1 p_y^1 p_z^1$), the resulting electronic configuration would be consistent with that of IXs. The octagonal ring VIII, unlike the trimer, can be viewed as a rhombic Al_4 with As atoms bridged at each side. This D_{2d} structure is labeled VIIIs and has a $^1A_1$ ground state with energy 0.93 eV above the minimum energy isomer. In this configuration, the Al–Al and Al–As distances are 2.993 Å and 2.316 Å, respectively. The Al–As–Al angle is 80.5° and the As–Al–As angle is 179.7°. The electronic configuration is {core} $(a_1)^2 (e)^4 (b_2)^2 (a_1)^2 (b_1)^2 (e)^4 (e)^4 (b_2)^2 (a_2)^2 (b_2)^2 (e)^4 (a_1)^2$. The triplet state is obtained upon $10a_1 \rightarrow 11a_1$ excitation. This D_{2h} structure is labeled as VIIIt and has a ^3A_u electronic state. In order to assess the importance of aluminum–aluminum interaction, the Al–Al separation was increased while simultaneously decreasing the As–As distance. As with the trimer, the energy increases as these distances are changed and a stationary point (Xs) is located more than 2.37 eV above the minimum energy isomer. The singlet state electronic configuration is {core} $(a_1)^2 (e)^4 (b_2)^2 (b_2)^2 (a_1)^2 (b_1)^2 (e)^4 (a_1)^2 (e)^4 (b_2)^2 (a_1)^2 (e)^4$. The triplet state is obtained upon $28e \rightarrow 12b_2$ excitation. This C_2 structure is labeled as Xt and has a ^3B electronic state. The indication is that Al–Al interaction is significant and contributes to the stabilization of this geometry. On the properties of Si_8, Ga_4As_4 and Al_4P_4 clusters, no theoretical study has been devoted to these clusters at same level of theory, to the best of our knowledge. Therefore, we also explore the structures and energies of Si_8, Ga_4As_4 and Al_4P_4 clusters in the framework of density functional theory. DFT studies find that the structures and orbital configuration of Al_4As_4 (IXs) is analogous to those of the valence-isoelectronic Al_4P_4 clusters (Table 4). This result agrees with the expectation that AlAs clusters and AlP clusters would exhibit similarities.

3.2. Cluster stability and ionization potential

For the remainder of the discussion, we focus on the minimum energy structural isomers for each cluster size. These include one structure for the dimer (IIs), one isomer for the trimer (VIs) and one for the tetramer (IXs). The singlet–triplet energy differences for the most stable geometries are significant. Values of 2.00 eV, 1.03 eV and 0.38 eV, respectively, were calculated for the dimer, trimer and tetramer. These

large differences reflect the relative stability of the clusters to reaction. For the most stable isomers of Al_2As_2, Al_3As_3 and Al_4As_4, the atomization energies are 11.46 eV, 18.87 eV and 27.13 eV. The increasing atomization energies indicate that the formation of the clusters is a favorable process. If we restrict our consideration to only the clusters described in this letter, we obtain the possible fragmentation processes shown in Table 5 for spin-allowed reactions. The fragmentation energy for the minimum energy dimer cluster (IIs) corroborates the interpretation of this structure as an end-capped As_2, since the dissociation energy for production of As_2 and atomic aluminum is small. For these clusters (IIs, VIs and IXs), the $n = 2$ and 3 clusters would be expected to fragment by loss of a monomeric Al–As unit. However, for the $n = 4$ cluster, formation of dimeric

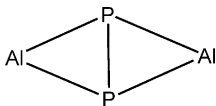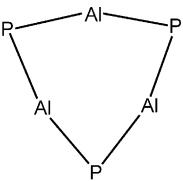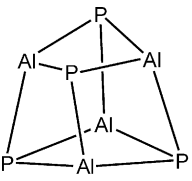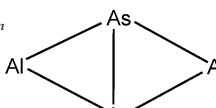Table 4
Geometric parameters for Al_nP_n [20] and Al_nAs_n
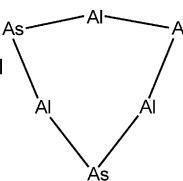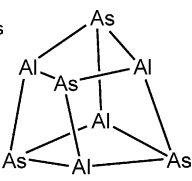
	$n = 2$	$n = 3$	$n = 4$
Al_nP_n	^1A_g (D_{2h} symmetry) r_{Al-P}=2.542 Å r_{P-P}=2.080 Å ∠Al-P-Al=131.7° ∠P-Al-P=49.3°	$^1A_1'$ (D_{3h} symmetry) r_{Al-P}=2.227 Å r_{Al-Al}=2.794 Å ∠Al-P-Al=77.7° ∠P-Al-P=162.3°	$^1T_2$ (T_d symmetry) r_{Al-P}=2.375 Å r_{Al-Al}=2.732 Å ∠Al-P-Al=70.2° ∠P-Al-P=106.7°
Al_nAs_n	^1A_g (D_{2h} symmetry) r_{Al-As}=2.662 Å r_{As-As}=2.309 Å ∠Al-As-Al=128.6° ∠Al-As As=64.3°	$^1A_1'$ (D_{3h} symmetry) r_{Al-As}=2.332 Å r_{Al-Al}=2.850 Å ∠Al-As-Al=75.3° ∠As-Al-As=164.7°	$^1T_2$ (T_d symmetry) r_{Al-As}=2.490 Å r_{Al-Al}=2.803 Å ∠Al-As-Al=68.5° ∠As-Al-As=107.8°

Table 5

Dissociation energetics for the aluminum arsenide clusters using CCSD(T)/6-311G(d,p) method

Structure	Reaction	Energy (eV)
IIs	$Al_2As_2 \rightarrow 2Al–As$ ($^3\Sigma$)	4.42
	$Al_2As_2 \rightarrow 2Al–As$ ($^1\Sigma$)	5.49
	$Al_2As_2 \rightarrow As_2$($^1\Sigma g$) + $2Al$(^2P)	4.23
VIs	$Al_3As_3 \rightarrow 3Al–As$ ($^1\Sigma$)	9.92
	$Al_3As_3 \rightarrow Al–As$ ($^1\Sigma$) + Al_2As_2 (^1A_g)	4.42
	$Al_3As_3 \rightarrow Al–As$ ($^3\Sigma$) + Al_2As_2 (^3B)	5.89
IXs	$Al_4As_4 \rightarrow 4Al–As$ ($^1\Sigma$)	15.20
	$Al_4As_4 \rightarrow Al–As$ ($^1\Sigma$) + Al_3As_3 ($^1A_1'$)	5.28
	$Al_4As_4 \rightarrow 2Al_2As_2$ (^1A_g)	4.21
	$Al_4As_4 \rightarrow 2Al_2As_2$ (^3B)	8.20

Table 6

Vertical ionization potentials of ground state clusters using CCSD(T)/6-311G(d,p) method

Cluster	Structure	Ionization energy (eV)
AlAs ($^3\Sigma$)		8.84
Al_2As_2 (^1A_g)	IIs	7.08
Al_3As_3 ($^1A_1'$)	VIs	8.98
Al_4As_4 ($^1T_2$)	IXs	8.03

units is expected to compete with this process. Vertical ionization potentials (single point calculations for the doublet ion using the optimized neutral geometry) are presented in Table 6.

3.3. Frequencies

The harmonic vibrational frequencies of the lowest energy isomer for each cluster were calculated and are presented in Table 2. The dimer (IIs) has three infrared active modes. The trimer (VIs) and tetramer (IXs) each have seven and nine IR active vibrational modes. For cluster IIs and VIs, one mode (b_{1u} for the dimmer, e' for the trimer) is an in plane motion and this vibration is predicted to exhibit the highest spectral intensity. The out-of-plane modes are very low in frequency. The remaining IR active vibrations, all of which exhibit moderate spectral intensities, are of b_{2u} or a_2'' symmetry and represent in plane distortion of the ring. IR active vibrational modes of the tetramer (IXs) are of t_2 symmetry and represent distortion of the cubic form. We consider dimmer (IIs) separately. This cluster has the same frequencies as the other rhombic dimmer, but the energies are quite different. Most importantly, the a_g stretch, which occurs along the short As–As axis, is indicative of the strong bonding interaction in this direction.

4. Conclusions

Our systematical calculation using density functional theory on singlet and triplet Al_nAs_n ($n = 1$–4) potential surfaces reveal that the ground state structures for both Al_2As_2 and Al_3As_3 are planar cumulenic rings with D_{2h}(^1A_g) and D_{3h}($^1A_1'$) symmetry, respectively. For Al_4As_4, a caged structure as observed in Si_8 and Al_4P_4 clusters is predicted as the most stable structure. The

loss of a AlAs monomer is shown to be the most likely fragmentation channel for many isomers. Comparisons with valence-isoelectronic Si_{2n}, Al_nP_n and Ga_nAs_n clusters of same size, the properties of the aluminum arsenide clusters are analogous to those of their corresponding Al_nP_n, Si_{2n} counterparts. The knowledge of the physical and chemical properties of these materials at the molecular level can be vital in explaining the mechanism of the modification and refinement, such as the modification and refinement of Si phase in Al–Si alloy. In addition, this method can act as a new way to find modifying agent and refining agent and shorten the working time and reduce cost of experimental material.

References

[1] K. Raghavachari, J. Chem. Phys. 84 (10) (1986) 5672.
[2] W. Kratschmer, L.D. Lamb, K. Fostiropoulos, D.R. Huffman, Nature 347 (1990) 354.
[3] K.D. Kolenbrander, M. Mandich, J. Chem. Phys. 92 (1990) 4759.
[4] Z.Y. Liu, C.R. Wang, R.B. Huang, L.S. Zheng, Int. J. Mass Spectrom. Ion Processes 141 (1995) 201.
[5] G.W. Lemire, G.A. Bishea, S.A. Heidecke, M.D. Morse, J. Chem. Phys. 92 (1990) 121.
[6] C. Jin, K.T. Taylor, J. Conceicao, R.E. Smalley, Chem. Phys. Lett. 175 (1990) 17.
[7] K. Balasubramanian, Chem. Phys. Lett. 171 (1990) 58.
[8] U. Meier, S.D. Peyerimhoff, F. Grein, Chem. Phys. 150 (1991) 331.
[9] L. Lou, L. Wang, L. Chibante, R.T. Laaksonen, P. Nordlander, R.E. Smalley, J. Chem. Phys. 94 (1991) 8015.
[10] M.A. Al-Laham, K. Raghavachari, Chem. Phys. Lett. 187 (1991) 13.
[11] L. Lou, P. Nordlander, R.E. Smalley, J. Chem. Phys. 97 (1992) 1858.
[12] M.A. Al-Laham, G.W. Trucks, K. Raghavachari, J. Chem. Phys. 96 (1992) 1137.
[13] W. Andreoni, Phys. Rev. B. 45 (1992) 4203.
[14] D.W. Liao, K. Balasubramanian, J. Chem. Phys. 96 (1992) 8938.
[15] P. Piquini, S. Canuto, A. Fazzio, Int. J. Quant. Chem. 28 (1994) 571.
[16] A. Tomasulo, M.V. Ramakrishna, J. Chem. Phys. 105 (1996) 10449.
[17] P.Y. Feng, K. Balasubramanian, Chem. Phys. Lett. 258 (1996) 387.
[18] P. Korambath, S.P. Karna, J. Chem. Phys. 104 (2000) 4801.
[19] H. Quck, Y. Feng, C.Z. Ong, Phys. D 42 (1997) 309.
[20] Y. Qu, X. Bian, J. Comput. Chem. 26 (2005) 226–234.
[21] A.K. Kandalam, M.A. Blanco, R. Pandey, J. Phys. Chem. B 105 (2001) 6080.
[22] K. Kolenbrander, M.L. Mandich, J. Chem. Phys. 92 (1990) 4659.
[23] C. Xu, E. de Beer, D.W. Arnold, C.C. Arnold, D.M. Neumark, J. Chem. Phys. 101 (1994) 5406.
[24] J.J. BelBruno, Chem. Phys. Lett. 313 (1999) 795–804.
[25] K.R. Asmis, T.R. Taylor, D.M. Neumark, Chem. Phys. Lett. 308 (1999) 347.
[26] A. Sutjianto, R. Pandey, J.M. Recio, Int. J. Quant. Chem. 52 (1994) 199.
[27] C.D. Purvis, R.J. Bartlett, J. Chem. Phys. 76 (1982) 1910.
[28] K. Raghavachari, G.W. Trucks, J.A. Pople, M. Head-Gordon, Chem. Phys. Lett. 157 (1989) 479.
[29] J.M.L. Martin, J. El-yazal, J.P. Francis, R. Gijbels, Chem. Phys. Lett. 232 (1995) 289.
[30] J.M.L. Martin, J. El-yazal, J.P. Francis, R. Gijbels, Chem. Phys. Lett. 248 (1996) 95.
[31] P.Y. Feng, K. Balasubramanian, Chem. Phys. Lett. 258 (1996) 387.

[32] P. Korambath, S.P. Karna, J. Chem. Phys. 104 (2000) 4801.

[33] T.R. Taylor, K.R. Asmis, C. Xu, D.M. Neumark, Chem. Phys. Lett. 297 (1998) 133.

[34] A.F. Belyanin, L.L. Bouilov, V.V. Zhirnov, A.I. Kamemev, K.A. Kovalskij, B.V. Spitsyn, Diamond Relat. Mater. 8 (1999) 369.

[35] A.D. Becke, J. Chem. Phys. 98 (1993) 5648.

[36] A.D. Becke, Phys. Rev. A 38 (1988) 3098.

[37] C. Lee, W. Yang, R.G. Parr, Phys. Rev. B 37 (1988) 785.

[38] B. Miehlich, A. Savin, H. Stoll, H. Preuss, Chem. Phys. Lett. 157 (1989) 200.

[39] R. Krishnan, J.A. Pople, Int. J. Quant. Chem. 14 (1978) 91.

[40] R. Krishnan, M.J. Frisch, J.A. Pople, J. Chem. Phys. 72 (1980) 4244.

[41] J.E. Carpenter, F. Weinhold, J. Mol. Struct. (Theochem) 169 (1988) 41.

[42] J.E. Carpenter, Ph.D. Thesis, University of Wisconsin, Madison, WI, 1987.

[43] J.P. Foster, F. Weinhold, J. Am. Chem. Soc. 102 (1980) 7211.

[44] A.E. Reed, F. Weinhold, J. Chem. Phys. 78 (1983) 4066.

[45] A.E. Reed, F. Weinhold, J. Chem. Phys. (1983) 1736.

[46] A.E. Reed, R.B. Weinstock, F. Weinhold, J. Chem. Phys. 83 (1985) 735.

[47] A.E. Reed, L.A. Curtiss, F. Weinhold, Chem. Rev. 88 (1988) 899.

[48] F. Weinhold, J.E. Carpenter, Plenum (1988) 227.

[49] J.P. Foster, F. Weinhold, J. Am. Chem. Soc. 102 (1980) 7211.

[50] A.E. Reed, R.B. Weinstock, F. Weinhold, J. Chem. Phys. 84 (1986) 2428.

[51] E. Kaufmann, K. Raghavachari, A.E. Reed, P.V.R. Schleyer, Organometallics 7 (1988) 1597.

[52] M.J. Frisch, G.W. Trucks, H.B. Schlegel, G.E. Scuseria, M.A. Robb, J.R. Cheeseman, J.A. Montgomery Jr., T. Vreven, K.N. Kudin, J.C. Burant, J.M. Millam, S.S. Iyengar, J. Tomasi, V. Barone, B. Mennucci, M. Cossi, G. Scalmani, N. Rega, G.A. Petersson, H. Nakatsuji, M. Hada, M. Ehara, K. Toyota, R. Fukuda, J. Hasegawa, M. Ishida, T. Nakajima, Y. Honda, O. Kitao, H. Nakai, M. Klene, X. Li, J.E. Knox, H.P. Hratchian, J.B. Cross, C. Adamo, J. Jaramillo, R. Gomperts, R.E. Stratmann, O. Yazyev, A.J. Austin, R. Cammi, C. Pomelli, J.W. Ochterski, P.Y. Ayala, K. Morokuma, G.A. Voth, P. Salvador, J.J. Dannenberg, V.G. Zakrzewski, S. Dapprich, A.D. Daniels, M.C. Strain, O. Farkas, D.K. Malick, A.D. Rabuck, K. Raghavachari, J.B. Foresman, J.V. Ortiz, Q. Cui, A.G. Baboul, S. Clifford, J. Cioslowski, B.B. Stefanov, G. Liu, A. Liashenko, P. Piskorz, I. Komaromi, R.L. Martin, D.J. Fox, T. Keith, M.A. Al-Laham, C.Y. Peng, A. Nanayakkara, M. Challacombe, P.M.W. Gill, B. Johnson, W. Chen, M.W. Wong, C. Gonzalez, J.A. Pople, Gaussian 03, Revision 6.0, Gaussian, Inc., Pittsburgh, PA, 2003.